

# Anisotropic molecular movements in organic crystals by mechanical stress

Gerd Kaupp,<sup>1\*</sup> Jens Schmeyers<sup>1</sup> and Ude D. Hangen<sup>2</sup>

<sup>1</sup>University of Oldenburg, Organic Chemistry I, POB 2503, D-26111 Oldenburg, Germany

<sup>2</sup>Surface Nano-Lab, Rheinstrasse 7, D-41836 Hückelhoven, Germany

Received 19 November 2001; revised 17 December 2001; accepted 24 January 2002

## epoc

**ABSTRACT:** Nanoindenters and nanoscratching on organic crystals with their anisotropic molecular packing explore far-reaching molecular movements or abrasion of material by the application of mechanical stress. Only intermolecular hydrogen bonds and van der Waals 'bonds' are broken in these experiments. Thiohydantoin (**1**) is a particularly suitable model owing to its well-defined layered crystal packing and its cleavability at the (10–2)-planes. Indents with a cube corner indenter on the natural (110)-face give piling-up of material by molecular movements only to one side by following the direction of the slopes of the molecular monolayers. Four orthogonal nanoscratches along and across the long crystal edge (each back and forth) on (110) give four different very distinct results: (1) molecular movements to both sides and in front with symmetric piling-up, (2) abrasion of material, (3) molecular movements to the right and (4) molecular movements to the left. The influence of the single molecular layers that stand 66° steep is clearly expressed by these results. No molecular movement but abrasion of material occurs upon nanoscratching on the (10–2) cleavage plane of **1**, now with the molecular monolayers flat. These anisotropic molecular responses to mechanical stress are detected by atomic force microscopy. They may be of use in nanotechnology, but cannot be predicted by the more common collective mechanical properties such as hardness or Young's elasticity modulus, quantities that do not at all relate to the extreme anisotropies that are reported here for the first time. Copyright © 2002 John Wiley & Sons, Ltd.

Additional material for this paper is available from the epoc website at <http://www.wiley.com/epoc>

**KEYWORDS:** anisotropic molecular movements; atomic force microscopy; hydrogen bonds; nanoindenter; nanoscratches; organic crystal

## INTRODUCTION

Anisotropic deformations upon mechanical stress by (nano)indentation of organic crystals have not been reported. They are known in the case of inorganic and polymer materials and have been interpreted as 'plastic deformation,' 'flow,' 'some kind of sliding,' 'cracks along shearing/cleaving planes,' 'local morphological changes' and the like.<sup>1,2</sup> For crystals of organic molecules, the possibility of long-range molecular movements should be envisaged as these occur and are required in their chemical reactions.<sup>3</sup> Such molecular movements have been unambiguously detected by atomic force microscopy (AFM) and near-field optical microscopy (SNOM)<sup>3</sup> and by grazing incidence diffraction (GID).<sup>4</sup> Anisotropic molecular migrations were not expected by the apparently still common topochemistry hypothesis,<sup>3</sup> which claimed 'minimal atomic and molecular movements' in solid-state chemical reactions. It was therefore of interest to examine the behavior of organic crystals

under the action of mechanical stress if no chemical transformations occur, except the breakage of intermolecular hydrogen bonds. Regular AFM tips are not able to achieve long-range molecular movements with formation of surface features. However, controlled abrasion of material was obtained with off-axis cantilever tips on organic crystals that consisted of three-dimensionally interlocked immobile molecules.<sup>5</sup> In these AFM scratching experiments the applied force is not normal to the surface. Reliable mechanical nanotesting requires normal force and thus the setup of a nanoindenter with transducer and linearly variable forces. We report on the first long-range anisotropic molecular movements in an organic crystal that were achieved solely by mechanical stress.

## RESULTS AND DISCUSSION

### Nanoindenters

Thiohydantoin (**1**) crystals ( $P2_1/c$ )<sup>6</sup> were chosen because they exhibit clear packing anisotropies on their natural (110)-face and cleave along the (10–2)-face. Molecules or

\*Correspondence to: G. Kaupp, Universität Oldenburg, Organische Chemie I, Postfach 2503, D-26111 Oldenburg, Germany.  
E-mail: kaupp@kaupp.chemie.uni-oldenburg.de

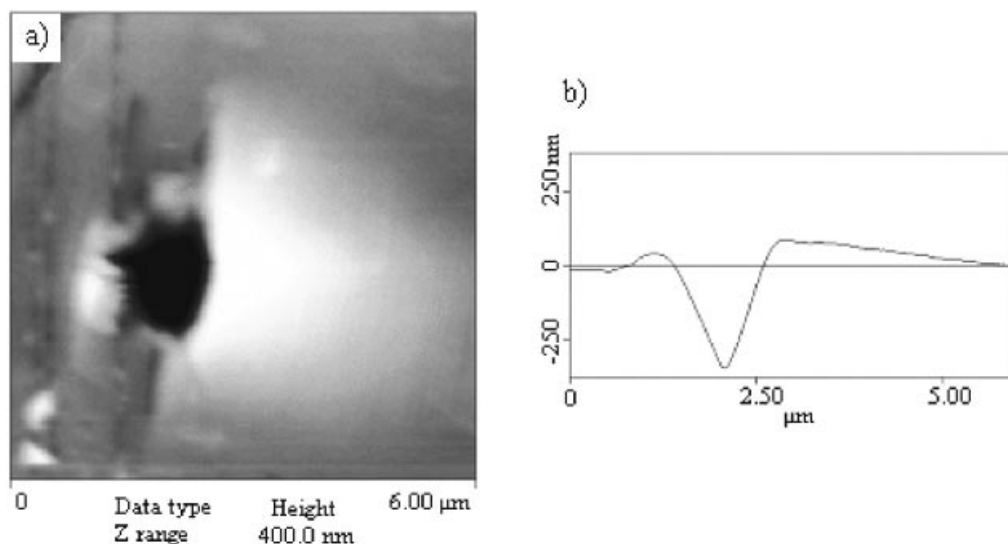


**Figure 1.** (a) AFM image of a nanoindent on the (110)-face of **1**; much more material is piled up to the right side of the depression than on the left side. (b) A horizontal cross-section through the center of the crater. The long edge of the crystal runs horizontally. High- and low-resolution VRML images of (a) are available at the epoc website at <http://www.wiley.com/epoc>

hydrogen-bridged aggregates of molecules may most easily move along cleavage planes, as has already been shown in cases of stress caused by geometric changes after chemical reactions, when **1** reacted with gaseous methyl- or dimethylamine in the absence of solvents or liquid phases.<sup>7</sup> As expected, anisotropic transport of materials can indeed be obtained by nanoindentation experiments on the (110)-face of **1**: the deep nanoindent (Fig. 1) piles up the displaced material on one side of the calibrated cube corner indenter. The piled-up volume ( $0.298 \mu\text{m}^3$ ) is larger than the volume of the depression ( $0.170 \mu\text{m}^3$ ), [various explanations have been put forward for such cases]<sup>8</sup> a fact that certainly relates to the cracking step formation (vertical to the long crystal edge) that occurred upon deformation and is depicted in Fig. 1(a). The unusual anisotropy is apparently caused by molecular movements under the (110)-surface that occur only in one direction. The piled-up hill is nearly axially symmetric with an ascending angle above the surface level at its steep side of  $<28^\circ$  and extending over more than  $4 \mu\text{m}$  with a uniform slope of  $1.5\text{--}2^\circ$  (Fig. 1). The orientation of the three faces of the cube corner indenter is clearly seen. The applied angle of  $45^\circ$  is almost reached at the right slope under the surface level of Fig. 1(b) (up to  $38^\circ$ ) where the molecules exit, while the slope at the left side (up to  $29^\circ$ ) is smaller, because the molecules could not exit there. The crystal packing of **1**<sup>6,7</sup> on the (110)-face is depicted in Fig. 2. The parallel monolayer sheets are  $66^\circ$  skew under the (110)-face. The infinite sheets are formed by two types of hydrogen bonds. However, there are no hydrogen bonds between the sheets. Thus, the crystal may be cleaved parallel to these sheets.

The unusual piling-up of material only at one side of

the indent must be caused by the skew cleavage planes under the (110)-face. The geometric arrangement in that experiment is sketched in Fig. 3(a). Clearly, the left side gaps between the sheets are blocked, as the indenter tip goes down. However, molecules or small H-bridged aggregates of them may exit at the right side even though the sheets will be bent to the right. Therefore, the pressure is translated further and released to the right by molecular movements above the surface. Figure 1(a) exhibits an indent with a maximum depth of 350 nm and indicates that the mechanical stress and the molecular migrations end at about a  $4 \mu\text{m}$  distance. The occurrence of cracks at the left side of Fig. 1 and the unequal volumes require additional support for that interpretation by the versatile new technique of nanoscratching at linearly increasing load.

### Nanoscratching on the (110)-face of thiohydantoin (**1**)

Nanoscratching experiments were performed on the (110)-face of **1** in four orthogonal directions with four different results that are depicted in Fig. 4. The scratch tests in Fig. 4(e) and (f) [see Fig. 3(b)] are depicted for a different crystal of **1** and at a 2.5 times higher load (1.9 times deeper) in order to show the robustness of the technique towards changes in the experimental conditions. The scratch along the long crystal edge following the sloping of the monolayer sheets in Fig. 4(a) [see Fig. 3(a)] gives molecular migrations in both directions of the cleavage planes with numerous cracks to both sides and translation to the front. The molecular migrations in both

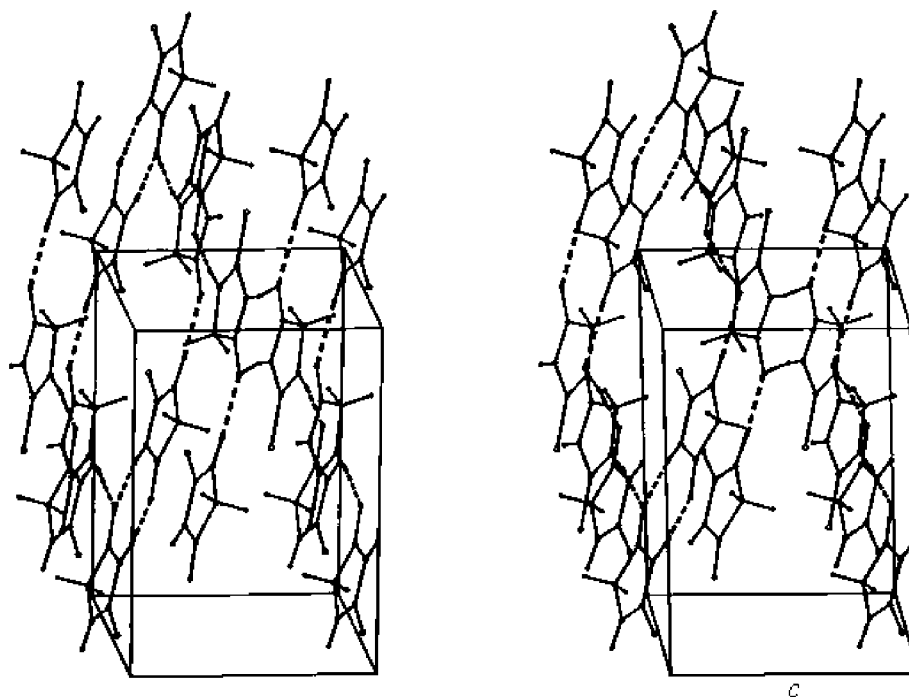
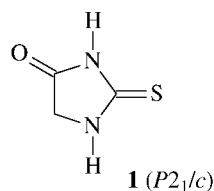


**Figure 2.** Stereoscopic representation of the molecular packing of **1** on its (110)-face showing monolayers with H-bridges; the hydrogen bridges (2.022 and 2.097 Å) are highlighted by dotted lines; the sheets/cleavage planes are perpendicularly oriented to the long crystal edge

directions (left and right) are clearly shown in Fig. 4(a) and in the cross-section of Fig. 4(c). As overhangs are formed, the apparent volume of piled-up material is

considerably higher than the volume of the depression and AFM cannot reasonably determine the ratio in this case. However, it appears that no material is lost by

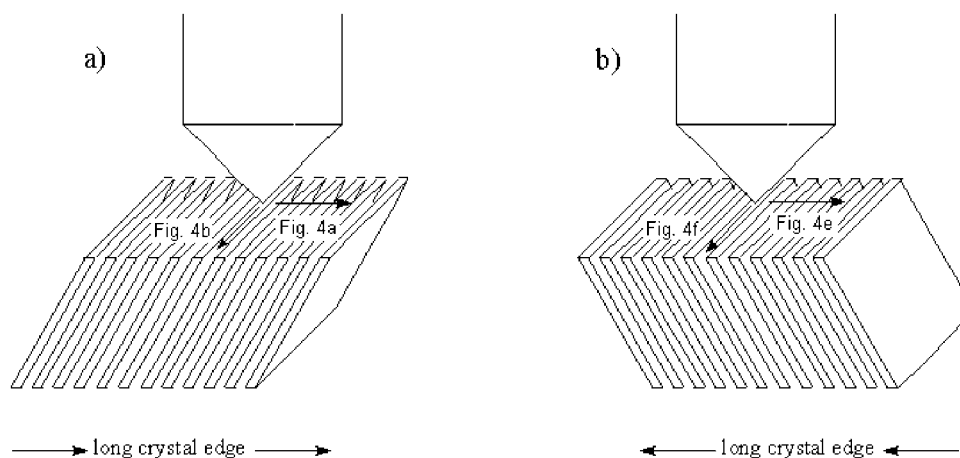


**Figure 3.** Geometric conditions for the mechanical tests with the vertical force of the indenter as applied to the (110)-face of **1**. (a) Skew sheets/cleavage planes sloping to the right by 66°. (b) Same crystal model turned by 180° around the vertical axis. The scratch directions in Fig. 4 are indicated

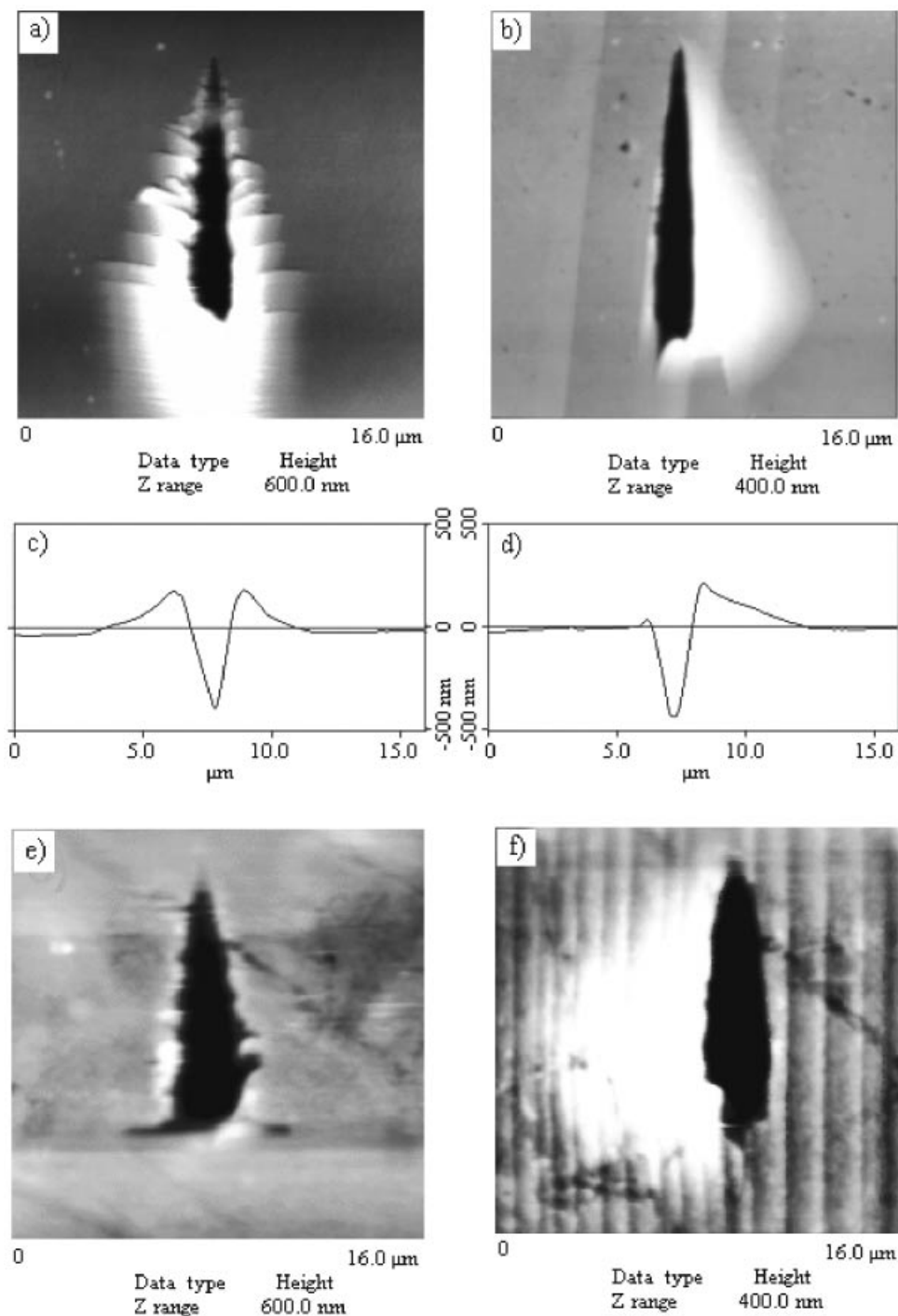


**Figure 4.** AFM micrographs of the scratch tracks on the (110)-face of **1**. (a) Following the skewed layers. (b) Along the cleavage planes sloping to the right. (c) Horizontal cross-section at the broadest width in (a). (d) Horizontal cross-section at the broadest width in (b). (e) Scratch against the sloping of the skew layers. (f) Scratch along the cleavage planes sloping to the left. A 400 μN final load was applied in (a) and (b) and 1000 μN in (e) and (f); the orientations are depicted in Fig. 3(a) and (b). High- and low-resolution VRML images of (a), (b), (e) and (f) are available at the epoc website at <http://www.wiley.com/epoc>

abrasion. On the contrary, the scratch in Fig. 4(e) against the sloping of the steep layers [see Fig. 3(b)] gives almost complete abrasion of material and only a very minor (4%) amount of pile-up. The material is lost

presumably as fine dust that can be pushed away by the AFM tip.<sup>5,9</sup>

Even more exciting is the scratch along the skew cleavage planes in Fig. 4(b) [see Fig. 3(a)]. The piling-up

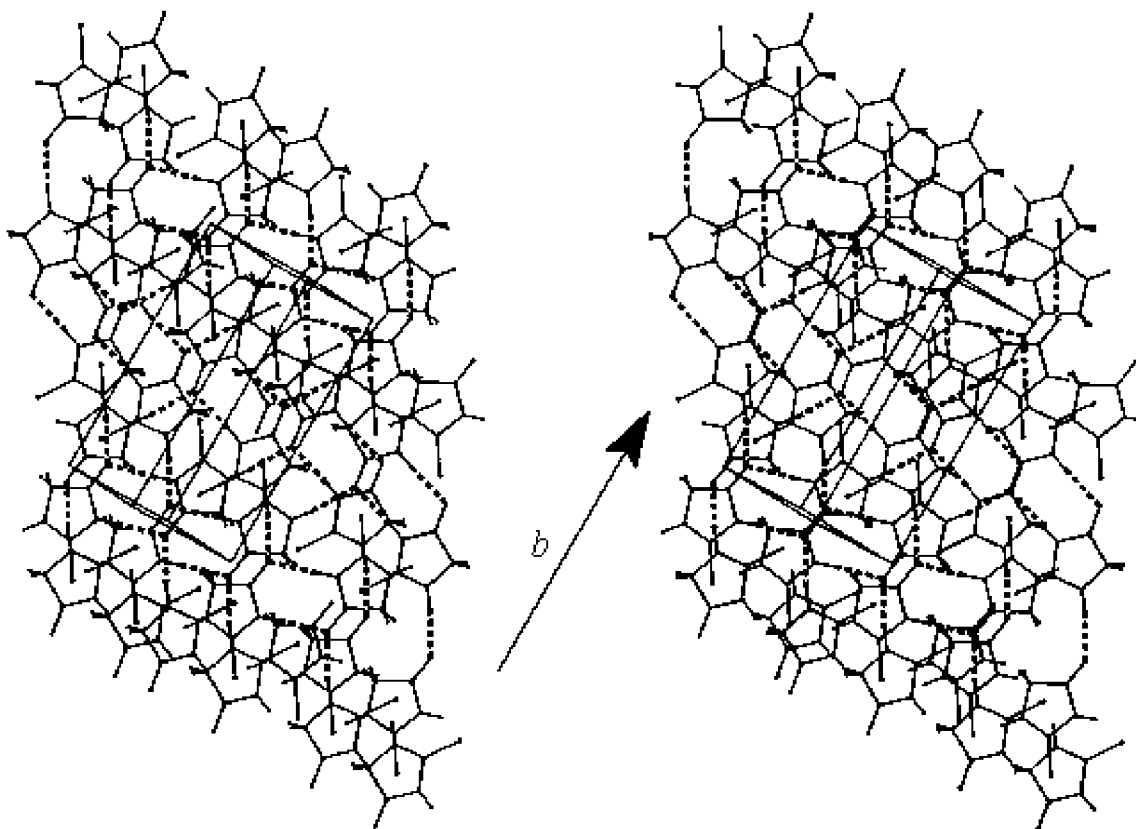


**Figure 5.** Stereoscopic surface model of **1** on the (10–2)-face with hydrogen-bridged sheets that are parallel to that face; the (010)- and (110)-faces are at the inclined top and to the left, respectively

of material occurs to the right image side exclusively and the volumes of pile-up ( $2.661 \mu\text{m}^3$ ) and ditch ( $2.588 \mu\text{m}^3$ ) are found to be equal. Clearly, the molecules can only move and exit at that side. This is also shown by the cross-section in Fig. 4(d). It is highly gratifying that the scratch along the cleavage planes in Fig. 4(f) [after a  $180^\circ$  turn of the crystal, see Fig. 3(b)] piled the migrating material to the left image side, as expected, and again there was no loss of material ( $5.012$  versus  $5.277 \mu\text{m}^3$ ).

The extreme direction sensitivities of the piling-up of material are clear evidence for molecular movements along the cleavage planes, as they depend solely on the orientation of the crystal. The right-left selectivity derives from the fact that the molecules can only exit from the unblocked gaps between the layers, as is evident from Fig. 3. The comparison of the volumes of hills and depressions indicates that no material was lost in the scratch tests of Fig. 4(a), (b) and (f) while almost all material of the scratch in Fig. 4(e) went to dust.

### Nanoscratching on the (10–2)-face of thiohydantoin (**1**)

The unusual behavior on the (110)-face of **1** should not

exist on the (10–2)-face (Fig. 5) as the layers are parallel to that face, and indeed, if a cleaved crystal was scratched on its (10–2)-face totally different results ensued: molecular movements could not be detected (Fig. 6).

No molecular movements but abrasion of material occurred if the (10–2)-face of a crystal of **1** was exposed to the scratchtest (Fig. 6). Only Fig. 6(a) exhibits some minor piling-up of material (ca 10%) at the end of the scratch, while Fig. 6(b) essentially does not. Clearly, most of the material of the scratch traces in Fig. 6 is abraded in the form of dust<sup>5,9</sup> that is removed and not recorded by AFM. The minor differences in Fig. 6(a) and (b) cannot yet be conclusively derived from the packing in Fig. 5. For example, the packing anisotropies on the (10–2)-face make the parallel paired hydrogen bonds be hit at angles of  $46^\circ$  and  $14^\circ$  in the scratch of Fig. 6(a) and at  $44^\circ$  and  $76^\circ$  in that of Fig. 6(b). However, these differences cannot be assessed owing to the great number of hydrogen bonds in all of the differently oriented infinite sheets that are all parallel to the face. Thus, if a scratch is executed on the (10–2)-face of **1** no molecules or small molecular aggregates can escape and migrate from their sheets. Rather, abrasion in the form of dust particles is to be expected and the direction should be of minor importance, as observed. This behavior of flat

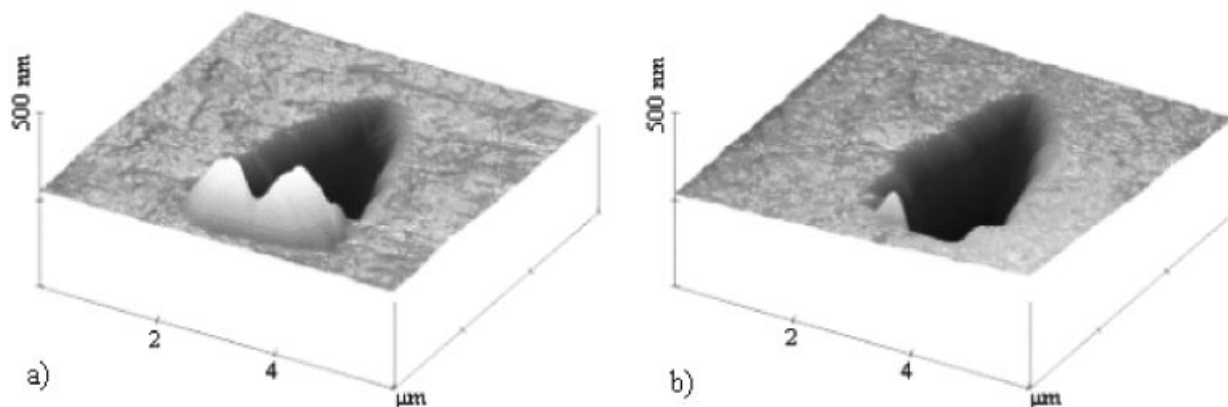


**Figure 6.** Perspective AFM views of the scratch tracks on the (10-2)-face of **1** with a final force of 1000  $\mu\text{N}$ . (a) Horizontal on the model in Fig. 5. (b) Vertical on the model in Fig. 5. High- and low-resolution VRML images of (a) and (b) are available at the epoc website at <http://www.wiley.com/epoc>

layers is totally different from that of steep layers under the (110)-face in Fig. 4.

### Mechanical properties

The marked differences in the anisotropic properties on the (110)- and (10-2)-faces of **1** are barely reflected in their collective mechanical properties that were determined by shallow indents (250 nm). Hardness and Young's reduced elasticity modulus were found to be 0.55 and 13.7 GPa on the (110)-face and 0.61 and 11.6 GPa on the (10-2)-face, respectively. The differences are small, although in the expected direction. Clearly, these collective mechanical properties do not relate well to anisotropies and the different uniform migrations.

### CONCLUSIONS

Mechanically induced molecular movements under the (110)-face of the crystals of **1** have been achieved. This is the first record of such an event that differs profoundly from anisotropic plasticities, e.g. of metals. The migrating molecules or small molecular aggregates must be liberated from infinite hydrogen-bonded layers. Thus, the tip that goes down vertically through the (110)-face in Fig. 2 apparently breaks hydrogen bonds just by mechanical interaction and enforces the covalently saturated fragments to migrate along the unobstructed cleavage planes. The regular shape of the hills that pile up either to the right or to the left side of the scratches in Fig. 4(b) and (f) indicate that full hydrogen bonding is reinstalled after the migration. Hydrogen-bond dimers, trimers or hexamers of **1** may be the most likely migrating species if not the isolated molecules. Extended parts of the 'infinite' sheets in **1** should not be able to migrate directionally owing to their bending away under the force of the

indenter tip and due to the action of huge numbers of van der Waals interactions. The energetics of the hydrogen bonds may be judged by density functional theory (DFT) calculations at the B3LYP/6-31 G\* level, although for gas-phase conditions. Every molecule of **1** exhibits three hydrogen bonds in the crystal. A trimer with all of the three different hydrogen bonds (the x-ray analysis has two of them at the same distance; Fig. 2) was chosen as a model. This trimer is by 22.2 kcal mol<sup>-1</sup> more stable than three isolated monomer molecules. The lengths of the hydrogen bonds were calculated as 1.875, 1.894 and 1.926 Å. Hence it may be concluded that less than 8 kcal mol<sup>-1</sup> is required to break mechanically a hydrogen bond in the crystal of **1**. This is certainly much less than the energetic requirement in the scratching of the standard out of fused quartz, that requires breakage of covalent Si—O bonds. Therefore, even the formation and migration of single molecules **1** appear energetically feasible during the scratching.

It is unusual that both extremes, complete piling-up of material or complete loss of material by abrasion, can be obtained with the same crystal upon indentation and scratching just by choosing different geometric alignments. Unlike chemically induced molecular movements in crystals that are driven by stress that is created by geometric changes,<sup>3,7</sup> the present results do not exhibit the complications of the molecular transformations. Numerous molecular migrations that occur in chemically reactive organic crystals<sup>3,7</sup> can now be analyzed in more detail. A new field of research is opened by the present findings and applications in nanotechnology, e.g. for surface structuring, can be envisaged.

### EXPERIMENTAL

The crystals of **1** were obtained as prisms from acetone. Their (110)-faces could be horizontally mounted. Flat

plates with (10–2)-faces were obtained by two parallel cleavages of the original crystals of **1**. The crystals were glued to the support of a Hysitron-TriboScope and tested with a calibrated cube corner diamond indenter tip (end radius 60 nm). The AFM imaging used a Digital Instruments 300 scanning probe microscope. Crystal packings were imaged with the program SCHAKAL 97 (E. Keller, University of Freiburg). Standard loading curves for the hardness and modulus determination were used at forces of 250  $\mu\text{N}$ . The load in the scratch tests was linearly increased to 400  $\mu\text{N}$  within a period of 30 s over a distance of 10  $\mu\text{m}$  [Fig. 4(a) and (b)] or to 1000  $\mu\text{N}$  [Fig. 4(e) and (f) and Fig. 6]. The cube corner indenter was aligned with one of its corners in front for the scratches. Estimates of the volumes of indents, scratches and piled-up materials were performed with the bearing analysis routine with respect to the plane through the left and the upper right corners of the 3D images. DFT calculations were performed with the program TITAN, version 1.01 (Wavefunctions, Irvine, CA, USA) and zero-point vibrational energy corrections were calculated with the program Jaguar 3.5, release 42 (Schrödinger, Portland, OR, USA).

### Supplementary material

The supplementary material available at the epoc website

at <http://www.wiley.com/epoc> contains the color images in GIF format and interactively usable full original 3D data of the images in VRML format in high and low resolution in order to allow for critical evaluation of the AFM results, their analytical use with suitable imaging software and future data mining. Interactive viewing is possible with public domain software, e.g. Cosmo Player or Blaxxun, via Internet Explorer.

### REFERENCES

1. Wolf B, Deus C, Paufler P. *Surf. Interface Anal.* 1997, **25**: 562–568.
2. Kempf M, Goeken M, Vehoff H. *Appl. Phys. A: Mater. Sci. Process.* 1998; **66**: 843–846; Bhushan B. *NATO ASI Ser., Ser. E* 1995, **286**: 367–395.
3. Kaupp G. In *Comprehensive Supramolecular Chemistry*, vol. 8, Davies JED, Ripmeester JA (eds). Elsevier: Oxford, 1996, 381–423.
4. Herrmann A, Kaupp G, Geue T, Pietsch U. *Mol. Cryst. Liq. Cryst.* 1997, **293**: 261–275.
5. Kaupp G, Schmeyers J, Pogodda U, Haak M, Marquardt T, Plagmann M. *Thin Solid Films* 1995, **264**: 205–211; Kaupp G, Plagmann M. *J. Photochem. Photobiol. A* 1994, **80**: 399–407.
6. Walker LA, Folting K, Merritt KL. *Acta Crystallogr., Sect. B* 1969, **25**: 88–93.
7. Kaupp G, Schmeyers J. *Angew. Chem., Int. Ed. Engl.* 1993, **32**: 1587.
8. Kaneko R, Hamada E. *Wear* 1993, **162–164**: 370–377; Han Y, Schmitt S, Friedrich K. *Appl. Composite Mater.* 1999, **6**: 1–18.
9. Bhushan B. *Proc. Inst. Mech. Eng.* 1998, **212** Part J: 1–18.